**Variation of mechanical and electrical performances of $Bi_2Ca_2Co_{1.7}O_x$ ceramics above working conditions**

Sh. Rasekh[1], M. Ghanbari[2], A. Natoli[3], M. A. Torres[4], M. A. Madre[4], A. Sotelo[4]

[1]CICECO – Aveiro Institute of Materials, Department of Materials and Ceramic Engineering, University of Aveiro, 3810-193 Aveiro (Portugal).

[2]Department of Electronics, Telecommunications and Informatics, University of Aveiro, 3810-193 Aveiro (Portugal).

[3]Department of Industrial Chemistry ‘‘Toso Montanari’’, Alma Mater Studiorum, Università Di Bologna, Viale Risorgimento 4, 40136 Bologna (Italy).

[4]ICMA (CSIC-Universidad de Zaragoza), C/María de Luna 3, 50018-Zaragoza (Spain).

**Abstract**

This work explores the effect of exposing the $Bi_2Ca_2Co_{1.7}O_x$ textured ceramics at temperatures above working conditions, on mechanical and electrical properties. Microstructural studies have shown a first improvement of microstructure with an important grain growth, followed by the formation of porosity and the appearance of cracks for larger times. These features were reflected on their mechanical and electrical properties. Three point bending tests have revealed an increase of bending strength with the thermal treatment, reaching the maximum at 24h and decreasing for further treatment time, which is very slight for times larger than 196h. On the other hand, electrical resistivity is drastically reduced with the thermal treatment when compared to the as-grown samples. Moreover, the samples behaviour is modified from semiconducting-like for as-grown samples to metallic-like for the thermally treated ones.

Accordingly, Seebeck coefficient is decreased with the thermal treatment, being very similar for all thermally treated samples. As a consequence of the drastic decrease of electrical resistivity, altough with lower reduction on the Seebeck coefficient, all thermally treated samples display higher power factor values than the as-grown ones. The highest values at 650 ºC (0.29 mW/ $K^2$ m) have been obtained in textured samples thermally treated for 48h, which are comparable to the best values reported in the literature without the use of expensive materials.

**Keywords:** Oxides; Texture; Aging; Mechanical properties; Electrical properties

## 1. Introduction

The current scarcity and high prices of fossil fuels, together with concerns about climate change caused by the emission of greenhouse gases, make the search for new technologies and more sustainable energy sources a priority for many countries. Nowadays there are numerous renewable energy sources (wind, hydroelectric, solar, etc.), although their use is limited by climatic conditions. Therefore, they still need the support of non-renewable energy sources (nuclear, coal, oil, etc.). Consequently, it is necessary to increase the efficiency of these non-renewable energy sources to reduce their fuel consumption and, in this way, decrease their emission of greenhouse gases and / or the waste heat produced in the energy transformation processes [1]. In this scenario, thermoelectric materials can play a critical role due to their ability to produce electrical energy from the heat wasted in these processes due to the Seebeck effect. The thermoelectric efficiency of these systems is determined by the dimensionless figure of merit, ZT, defined as $TS^2/\rho\kappa$. In this expression, T is the absolute temperature, S the Seebeck coefficient, $\rho$ the electrical resistivity, and $\kappa$ the thermal conductivity [2]. Currently, the practical applications of these systems are based on intermetallic materials, such as $CoSb_3$ or $Bi_2Te_3$, characterized by showing high ZT values at low or moderate temperatures [3,4]. However, the massive application of these systems to recover waste heat in classic energy transformation systems requires that they work at high temperatures, at which these intermetallic materials can oxidize, degrade, or even release, in some cases, heavy metals to the environment. However, the application temperature range of thermoelectric materials was expanded with the discovery of high thermoelectric characteristics in the $Na_2Co_2O_4$ ceramic system [5] which, in addition to being able to work at high temperatures, are based on abundant materials in the earth's crust [6,7]. This discovery marked the beginning of a great research activity on these ceramic materials, especially on the cobalt oxide based compounds [8,9]. Nevertheless, the properties of these materials must be further enhanced before they can be used in thermoelectric systems. One of the explored routes to improve them has been through their grain alignment to exploit their anisotropy [10]. The most common techniques used to align the grains in the bulk material are hot uniaxial pressing [11], spark plasma sintering (SPS) [12], template grain growth (TGG) [13], laser floating zone (LFZ) [14], and the electrically-assisted laser floating zone method (EALFZ) [15].

On the other hand, as these materials must work at high temperatures when they are integrated into thermoelectric modules, the evolution of their thermoelectric and mechanical properties must be known when subjected to high temperatures for long timespan. As a consequence, the objective of this work is studying the evolution of the thermoelectric and mechanical properties of $Bi_2Ca_2Co_{1.7}O_x$ when it is subjected to high temperatures, 800 ºC, for times up to 768 h. Their microstructural evolution will be evaluated, and related to their mechanical and thermoelectric properties.

## 2. Experimental

The initial $Bi_2Ca_2Co_{1.7}O_x$ ceramic precursors used in this work were prepared using $Bi_2O_3$ (≥ 99 %, Aldrich), $CaCO_3$ (≥ 98%, Aldrich), and CoO (99.99 %, Aldrich) commercial powders. They were weighed in the stoichiometric proportions, mixed, and ball milled in an agate ball mill at 300 rpm for 30 min in double distilled water. The suspension was subsequently dried using infrared radiation, and the powder mixtures

were thermally treated, in a two-step process, at 750 and 800 ºC for 12 h, with an intermediate manual milling. This thermal treatment has been proved necessary to decompose the $CaCO_3$ [16], which is of the main importance to avoid $CO_2$ bubbles formation during the texturing process. After calcination procedure, the powders were isostatically pressed in form of cylinders (~ 3 mm diameter) under 200 MPa which were used as feed in a LFZ system previously described [9]. All samples were grown at 30 mm/h, leading to textured cylindrical rods with slightly lower diameter than the initial one (between 2.5 and 2.8 mm). These textured rods were then subjected to long continuous thermal treatments at 800 ºC for times up to 768 h under air atmosphere.
Microstructural characterization has been made on longitudinal polished sections of samples in a Field Emission Scanning Electron Microscope (FESEM, Zeiss Merlin) equipped with an energy dispersive spectrometry (EDS) analysis system. Mechanical evaluation has been performed in an Instron 5565 machine, through the three-point bending tests. The measurements were made using a 10 mm loading span fixture, and a punch displacement speed of 30 μm/min. Electrical resistivity and Seebeck coefficient were simultaneously determined using the standard four-probe dc technique in a LSR-3 system (Linseis GmbH) working in steady state mode, between 50 and 650 ºC, under He atmosphere. With these data, power factor, PF (= $S^2/\rho$) has been calculated to evaluate the thermoelectric performances of samples.

## 3. Results and discussion

Fig. 1 shows SEM micrographs performed on polished longitudinal sections of samples using backscattered electrons. It is clear that all samples show a compact dense aspect with very low porosity, randomly distributed along the observed sections, as previously reported [16], while a good grains orientation along the growth direction can be seen. Moreover, the main observed differences between the as-grown sample (Fig. 1a) and the thermally treated ones (Fig. 1b-d) are the disappearance of the black dendritic contrast together with an increase of the thermoelectric grains sizes. Furthermore, these images show a higher amount of light grey phase in the inner part of the samples than on the edges. This is the typical situation when the samples possess an incongruent melting which leads to the formation of phases with very different melting point. Consequently, the center of these samples is enriched of the lowest melting point phase (such as Bi-Ca-O, light grey contrast) due to a radial solidification gradient, as reported for similar systems [17].

Fig. 2 shows representative SEM micrographs performed on the same zones of the samples. In these images, three different contrasts can be identified in as-grown samples (Fig. 2a), dark grey, light grey and dendritic black ones, associated through EDS to the thermoelectric $Bi_2Ca_2Co_{1.7}O_x$, $Bi_4Ca_3O_9$, and CoO phases, respectively. On the other hand, the CoO phase decreases with the thermal treatment, disappearing after only 48 h (see Fig. 2b). At the same time, the amount of the thermoelectric phase in the samples is higher when the duration of the thermal treatment is increased. This effect can be explained by the reaction between the different secondary phases, induced by the thermal treatment, to produce the thermoelectric one. Finally, other effect of the thermal treatment is related to the modification of the light grey contrast composition, which is Bi-enriched when the thermal treatment duration is raised.

Fig. 3 illustrates the flexural strength ($\sigma$) of samples, together with its standard error, as a function of the thermal treatment duration. As it can be observed in the plot, flexural strength increases around 15 % for samples with 48 h thermal treatment (130 MPa), when compared to the as-grown ones (110 MPa). Further thermal treatment leads to a gradual decrease to about 95 MPa for samples treated for 200 h, which is practically constant for larger times. The increase in $\sigma$ can be explained by the decrease in the secondary phases content and the cation diffusion between the grains which reinforces the grain boundaries and increases grain sizes, resulting in higher mechanical properties. On the other hand, when considering the microstructural evolution previously discussed, it should be expected that mechanical properties would be enhanced for larger thermal treatments. In order to determine the cause of this decrease of $\sigma$, microstructure of samples was deeply studied at high magnification, and the results of these observations are shown in Fig. 4. In the micrograph, the typical structure of these materials can be seen, consisting in plate-like grains stacked along their ab planes due to their preferential growth habit [18,19]. However, as it is well known, these grain possess weak grain boundaries along the c-direction which clearly influence the mechanical properties by the easy appearance of cracks along these grain boundaries, being more important when the grain sizes are increased. This fact is clearly illustrated by the large crack shown by arrows in Fig. 4.

Electrical resistivity variation with temperature for all samples is displayed in Fig. 5. As it is evident in the plot, all thermally treated samples show very similar behavior, maintaining the resistivity values practically unchanged in the whole measured temperature range. This behavior contrasts with that obtained in the as-grown samples, which show a marked semiconducting-like behavior ($d\rho/dT \leq 0$) up to about 550 ºC, and a slight metallic-like one at higher temperatures, in agreement with previous reports [20]. This different behavior can be explained by the decrease of secondary phases content during the thermal treatment, as well as to oxygen diffusion from the atmosphere to fill the high amount of oxygen vacancies produced by the laser texturing process [21]. These factors lead to higher oxygen content in the thermoelectric phase in the thermally treated samples, which increases the charge carrier concentration and decreases electrical resistivity. On the other hand, the slight differences found between the treated samples can be associated to the increase in charge carrier concentration with the processing time, and the growth of intergranular cracks due to the large grain growth with time. However, the effect of this last factor is very limited, as the cracks are parallel to the conducting planes of $Bi_2Ca_2Co_{1.7}O_x$ phase, explaining the evolution of electrical resistivity. The minimum resistivity values at 650 ºC (33 m$\Omega$ cm) have been determined in samples treated at 800 ºC for 24 h, which are very similar to the obtained in LFZ textured Pb-doped samples (32 m$\Omega$ cm) [20] and much lower than the reported for bulk sintered materials (70 m$\Omega$ cm) [18].

Fig. 6 shows the variation of the Seebeck coefficient with temperature obtained in all samples. As it can be easily observed, S values are positive at all temperatures, which correspond to p-type conduction mechanism, as dominant one. Moreover, they are increased with temperature, with very similar behavior for all samples. However, as-grown samples display higher values than the thermally treated ones. This behavior was expected, and it is in agreement with the previously discussed variation of charge carrier concentration, and described by Koshibae's expression [22], in which Seebeck coefficient decreases when the charge carrier concentration is increased. In any case, the highest values determined in these samples at 650 ºC (between 300 and 335 μV/K) are much higher than the reported in bulk sintered $Bi_2Ca_2Co_2O_y$ (235 μV/K) [23], laser textured (285 μV/K) [23], or single crystals (170 μV/K) [24].

Finally, using the ρ, and S data, the temperature dependence of PF has been calculated, and presented in Fig. 7, to determine the samples electrical performance. PF increases with temperature in all cases, showing a nearly linear trend. Moreover, all thermally treated samples display higher PF values than the as-grown ones in the whole measured temperature range provided by their much lower electrical resistivity. The highest PF values at 650 ºC have been determined in samples treated for 48 h (0.29 mW/K$^2$m), which are around 65 % higher than the obtained in as-grown materials. Moreover, they are higher than the reported in K-doped bulk and laser textured $Bi_2Ca_2Co_2O_y$ materials (0.11 mW/K$^2$m) [23], and comparable to the reported in Ag added materials (0.30 mW/K$^2$m) [25].

From these data, it is clear that the $Bi_2Ca_2Co_{1.7}O_y$ materials are promising candidates to be used in thermoelectric modules, as they can work for relatively long periods of time over the optimal working temperature, without drastic degradation of their electrical properties. However, mechanical properties degradation is still an issue to be deeply studied in order to avoid or, at least, limit their decrease over time within a reasonable range.

## 4. Conclusions

This work demonstrates that $Bi_2Ca_2Co_{1.7}O_y$ materials produced through the laser floating zone at relatively large growth rates can be subjected to higher temperatures than the optimal working ones without drastic lossess of performances along the time. Microstructural studies have revealed that as-grown samples are formed by two main secondary phases, besides the thermoelectric one, while thermally treated samples have higher content of the thermoelectric phase and only one secondary phase. Moreover, all samples present significant grain orientation, and relatively large grain sizes, which are increased with time under 800 ºC. Mechanical properties evaluated by the three point bending tests have shown an increase of around 15 % after 24 h thermal treatment, and a decrease of around 15 % after 768 h, when both are compared to the values obtained in as-grown samples. This evolution has been related to the thermoelectric grain growth which increases mechanical properties, and the fact that these grains tend to exfoliate by the formation of cracks along their stacking planes (ab-planes). Electrical resistivity has been drastically reduced for all samples, when compared to the as-grown ones, while Seebeck coefficient has been only slightly decreased. As a consequence, all thermally treated samples possess much higher power factor than the as-grown ones. The highest values at 650 ºC (0.29 $mW/K^2m$) are comparable to the obtained in Ag added materials, avoiding the use of expensive materials. These data point out to textured $Bi_2Ca_2Co_{1.7}O_y$ ceramics as promising materials for their integration in thermoelectric modules due to their ability to maintain their thermoelectric and mechanical properties within reasonable values when they are subjected to higher temperatures than the optimal working ones.

**Acknowledgements**

M. A. Torres, M. A. Madre, and A. Sotelo acknowledge the Spanish MINECO-FEDER (MAT2017-82183-C3-1-R) and Gobierno de Aragón-FEDER (Research group T54-20R), for financial support. Sh. Rasekh acknowledges the support of the Research Employment Contract FCT–CEECIND/02608/2017. Authors acknowledge the use of Servicio General de Apoyo a la Investigación-SAI, Universidad de Zaragoza.

## References

1. G. Mahan, B. Sales, J. Sharp, Thermoelectric materials: New approaches to an old problem, Phys. Today 50 (1997) 42–47.

2. D. M. Rowe, in Thermoelectrics handbook: macro to nano, ed. D. M. Rowe, CRC press, Boca Raton, FL, 2005.

3. H. Wang, J. Hwang, M. L. Snedaker, I.-H. Kim, C. Kang, J. Kim, G. D. Stucky, J. Bowers, W. Kim, High Thermoelectric Performance of a Heterogeneous PbTe Nanocomposite, Chem. Mater. 27 (2015) 944–949.

4. J. A. Santamaria, J. Alkorta, J. G. Sevillano, Microcompression tests of single-crystalline and ultrafine grain $Bi_2Te_3$ thermoelectric material, *J. Mater. Res.* 30 (2015) 2593–2604.

5. I. Terasaki, Y. Sasago, K. Uchinokura, Large thermoelectric power in $NaCo_2O_4$ single crystals, Phys. Rev. B 56 (1997) 12685–12687.

6. A. A. Yaroshevsky, Abundances of chemical elements in the Earth's crust. Geochem. Int. 44 (2006) 48–55.

7. J. He, Y. Liu, R. Funahashi, Oxide thermoelectrics: The challenges, progress, and outlook, J. Mater. Res. 26 (2011) 1762–1772.

8. F. Delorme, C. F. Martin, P. Marudhachalam, G. Guzman, D. O. Ovono, O. Fraboulet, Synthesis of thermoelectric $Ca_3Co_4O_9$ ceramics with high ZT values from a $Co^{II}Co^{III}$-Layered Double Hydroxide precursor, Mater. Res. Bull. 47 (2012) 3287–3291.

9. Sh. Rasekh, F. M. Costa, N. M. Ferreira, M. A. Torres, M. A. Madre, J. C. Diez, A. Sotelo, Use of laser technology to produce high thermoelectric performances in $Bi_2Sr_2Co_{1.8}O_x$, Mater. Design 75 (2015) 143–148.

10. R. Funahashi, I. Matsubara, H. Ikuta, T. Takeuchi, U. Mizutani, S. Sodeoka, An oxide single crystal with high thermoelectric performance in air, Jpn. J. Appl. Phys. 39 (2000) L1127–L1129.

11. H. Wang, X. Sun, X. Yan, D. Huo, X. Li, J.-G. Li, X. Ding, Fabrication and thermoelectric properties of highly textured $Ca_9Co_{12}O_{28}$ ceramic, *J. Alloys Compds.* 582 (2014) 294–298.

12. J. G. Noudem, D. Kenfaui, D. Chateigner, M. Gomina, Granular and Lamellar Thermoelectric Oxides Consolidated by Spark Plasma Sintering, J. Electron. Mater. 40 (2011) 1100–1106.

13. H. Itahara, C. Xia, J. Sugiyama, T. Tani, Fabrication of textured thermoelectric layered cobaltites with various rock salt-type layers by using $\beta$-$Co(OH)_2$ platelets as reactive templates, J. Mater. Chem. 14 (2004) 61–66.

14. M. A. Madre, F. M. Costa, N. M. Ferreira, S. I. R. Costa, Sh. Rasekh, M. A. Torres, J. C. Diez, V. S. Amaral, J. S. Amaral, A. Sotelo, High thermoelectric performance in $Bi_{2-x}Pb_xBa_2Co_2O_x$ promoted by directional growth and annealing, J. Eur. Ceram. Soc. 36 (2016) 67–74.

15. N. M. Ferreira, Sh. Rasekh, F. M. Costa, M. A. Madre, A. Sotelo, J. C. Diez, M. A. Torres, New method to improve the grain alignment and performance of thermoelectric ceramics, Mater. Lett. 83 (2012) 144–147.

16. Sh. Rasekh, M. A. Madre, A. Sotelo, E. Guilmeau, S. Marinel, J. C. Diez, Effect of synthetic methods on the thermoelectrical properties of textured $Bi_2Ca_2Co_{1.7}O_x$ ceramics, Bol. Soc. Esp. Ceram. V. 49 (2010) 89–94.

17. G. F. de la Fuente, M. T. Ruiz, A. Sotelo, A. Larrea, R. Navarro, Microstructure of laser floating zone (LFZ) textured (Bi,Pb)-Sr-Ca-Cu-O superconductor composites, Mater. Sci. Eng. A 173 (1993) 201–204.

18. A. Maignan, S. Hébert, M. Hervieu, C. Michel, D. Pelloquin, D. Khomskii, Magnetoresistance and magnetothermopower properties of Bi/Ca/Co/O and Bi(Pb)/Ca/Co/O misfit layer cobaltites, J. Phys. Condens. Matter. 15 (2003) 2711–2723.

19. H. Itahara, C. Xia, J. Sugiyama, T. Tani, Fabrication of textured thermoelectric layered cobaltites with various rock salt-type layers by using $\beta$-$Co(OH)_2$ platelets as reactive templates, J. Mater. Chem. 14 (2004) 61–66.

20. Sh. Rasekh, M. A. Madre, J. C. Diez, E. Guilmeau, S. Marinel, A. Sotelo, Effect of Pb substitution on the thermoelectrical properties of textured $Bi_2Ca_2Co_{1.7}O_x$ ceramics prepared by a polymer solution method, Bol. Soc. Esp. Ceram. V. 49 (2010) 371–376.

21. J. C. Diez, Sh. Rasekh, M. A. Madre, E. Guilmeau, S. Marinel, A. Sotelo, Improved thermoelectrical properties of Bi-M-Co-O (M=Sr, Ca) misfit compounds by laser directional solidification, J. Electron. Mater. 39 (2010) 1601–1605.

22. W. Koshibae, K. Tsuitsui, S. Maekawa, Thermopower in cobalt oxides, Phys. Rev. B Condens. Matter 62 (2000) 6869–6872.

23. C. Ozcelik, T. Depci, M. Gursul, G. Cetin, B. Ozcelik, M. A. Torres, M. A. Madre, A. Sotelo, Tuning thermoelectric properties of $Bi_2Ca_2Co_2O_y$ through K doping and laser floating zone processing, Solid State Sci. 120 (2021) 106732.

24. N. Sun, S. T. Dong, B. B. Zhang, Y. B. Chen, J. Zhou, S. T. Zhang, Z. B. Gu, S. H. Yao, Y. F. Chen, Intrinsically Modified Thermoelectric Performance of Alkaline-earth

Isovalently Substituted $[Bi_2AE_2O_4][CoO_2]_y$ Single Crystals, J. Appl. Phys. 114 (2013) 043705.

25. D. Flahaut, J. Allouche, A. Sotelo, Sh. Rasekh, M. A. Torres, M. A. Madre, J. C. Diez, Role of Ag in textured-annealed $Bi_2Ca_2Co_{1.7}O_x$ thermoelectric ceramic, Acta Mater. 102 (2016) 273–283.

**Figure captions**

**Figure 1.** Representative general views taken on longitudinal polished surfaces of $Bi_2Ca_2Co_{1.7}O_x$ ceramics subjected at 800 ºC for a) 0; b) 48; c) 192; and d) 768 h.

**Figure 2.** Representative general views taken on longitudinal polished surfaces of $Bi_2Ca_2Co_{1.7}O_x$ ceramics subjected at 800 ºC for a) 0; b) 48; c) 192; and d) 768 h. The arrows indicate the different composition associated to each contrast.

**Figure 3:** Flexural strength, together with its standard error, as a function of time under 800 ºC thermal treatment.

**Figure 4:** SEM micrograph of sample thermally treated for 768 h showing the appearance of cracks between the thermoelectric grains when their grain sizes are increased. The arrows show one of the large cracks formed in these samples.

**Figure 5:** Temperature dependence of the electrical resistivity for as-grown and thermally treated samples at 800 ºC for different timespan.

**Figure 6:** Temperature dependence of the Seebeck coefficient for as-grown and thermally treated samples at 800 ºC for different timespan.

**Figure 7:** Temperature dependence of the power factor for as-grown and thermally treated samples at 800 ºC for different timespan.

Figure 1

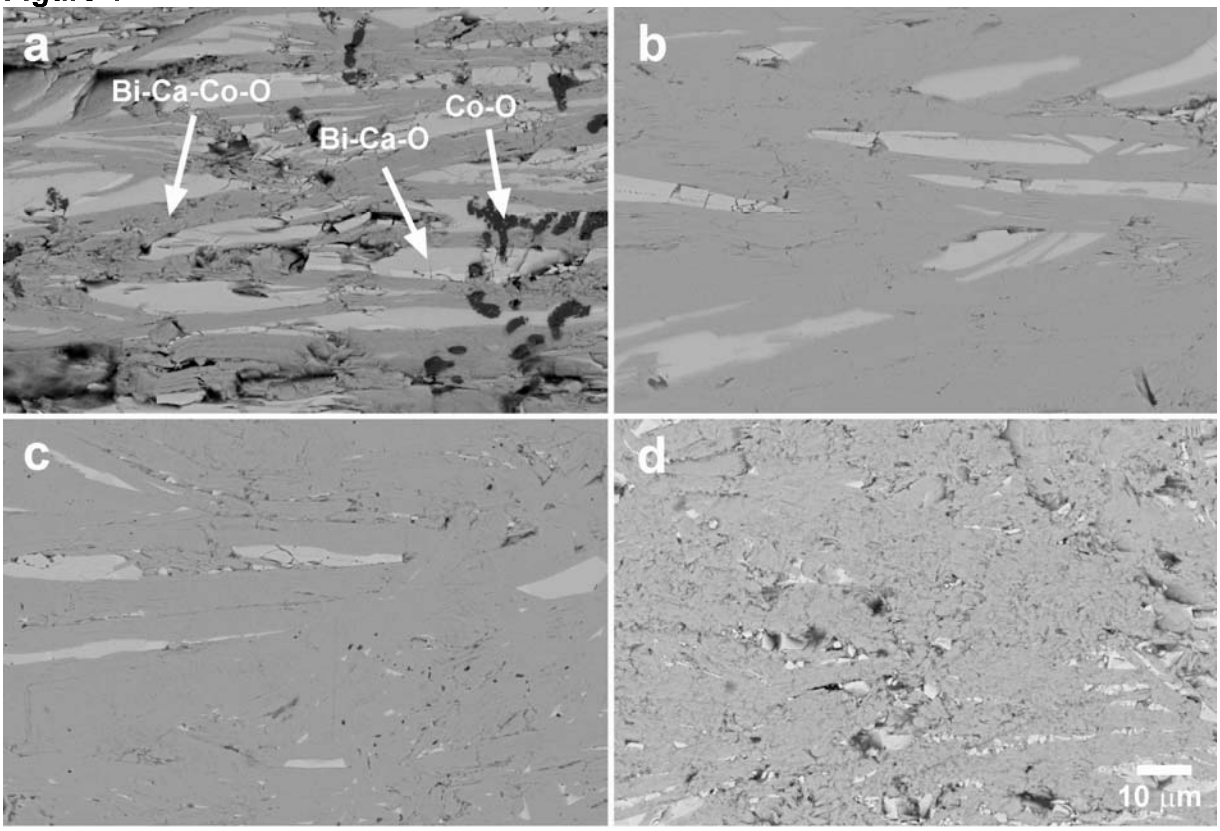

Figure 2

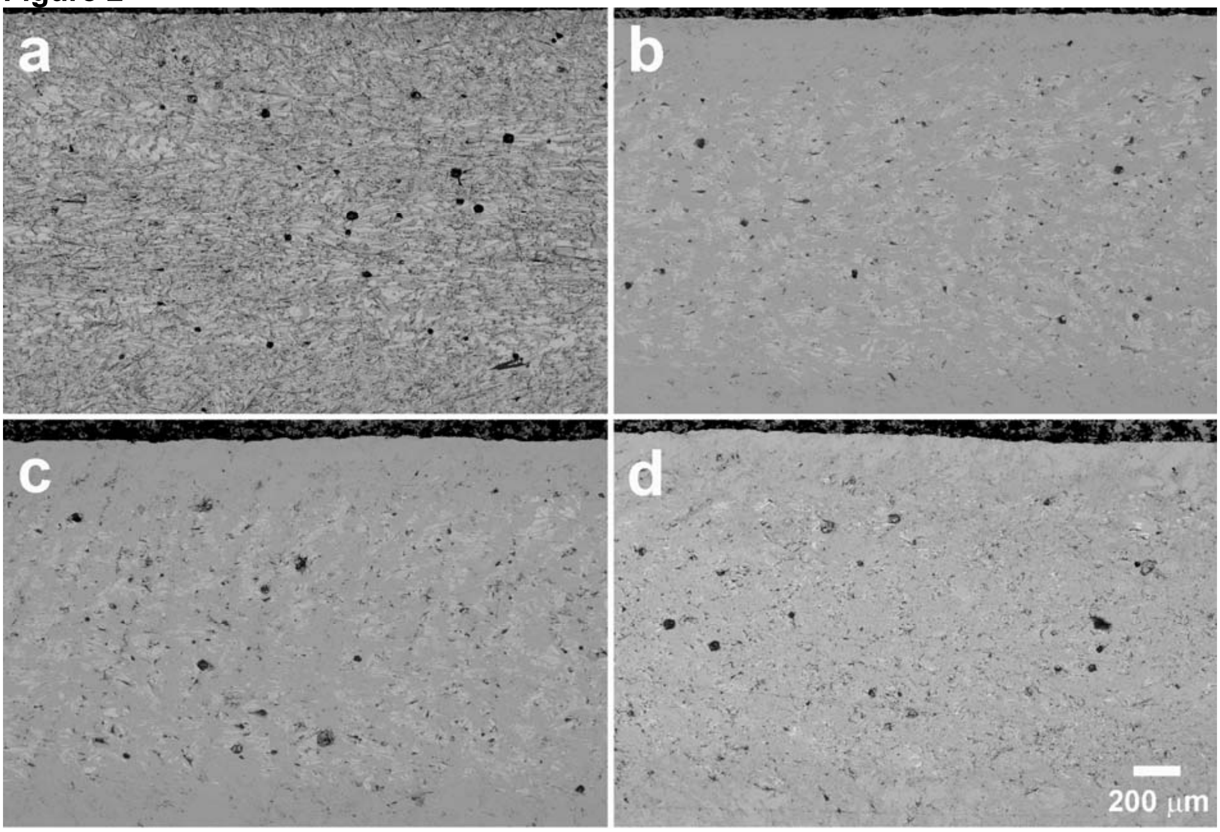

**Figure 3**

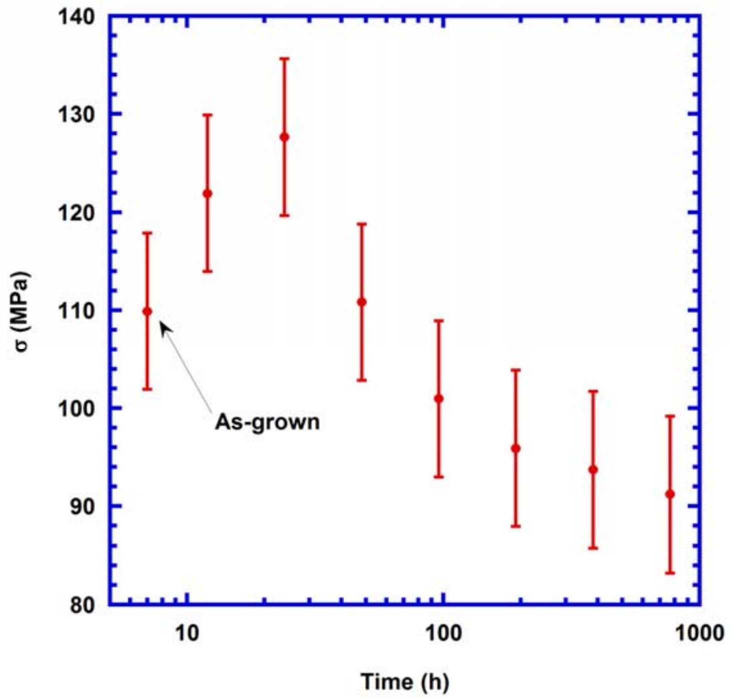

**Figure 4**

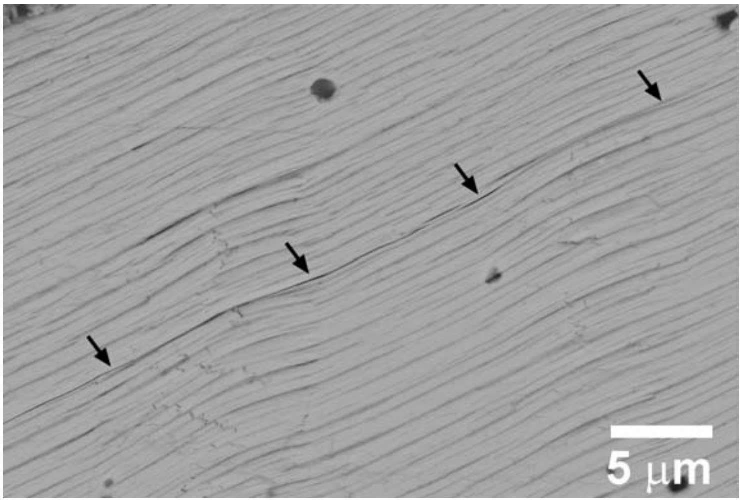

**Figure 5**

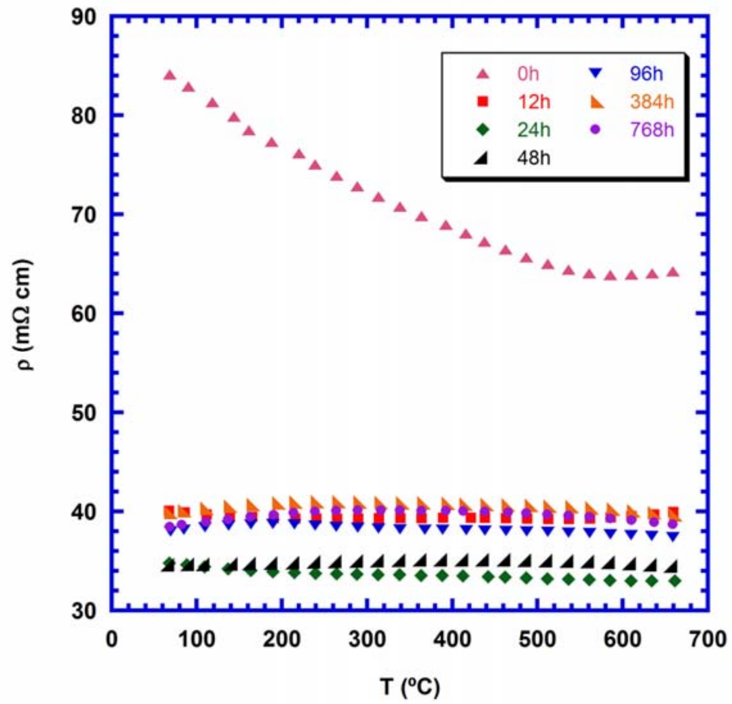

0h
96h
12h
384h
24h
768h
48h
ρ (mΩ cm)
T (ºC)
90
80
70
60
50
40
30
0
100
200
300
400
500
600
700

**Figure 6**

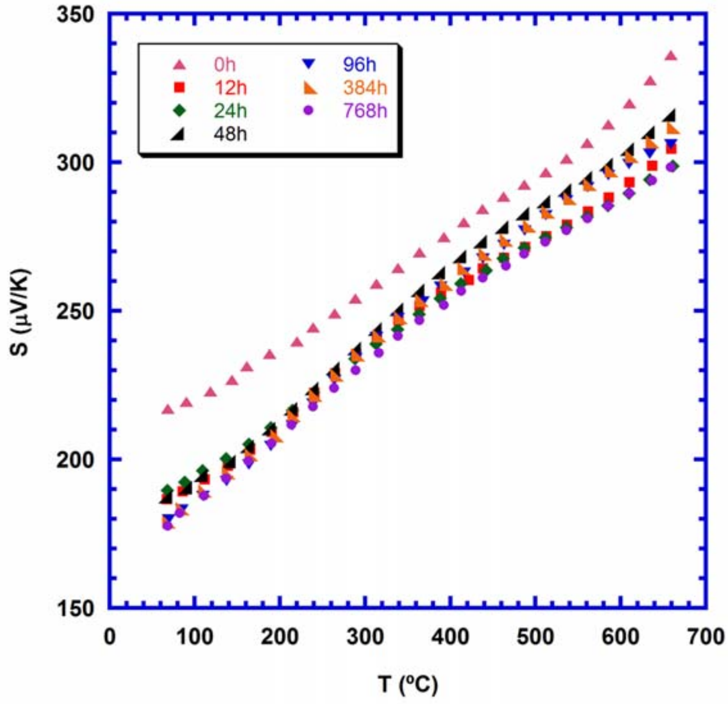

0h
12h
24h
48h
96h
384h
768h
S (μV/K)
T (ºC)
350
300
250
200
150
0
100
200
300
400
500
600
700

**Figure 7**

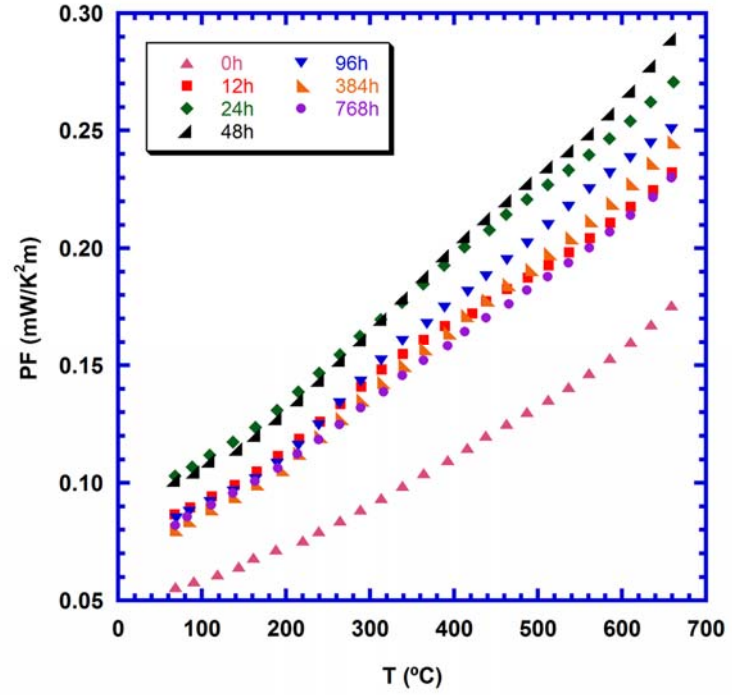

0h
12h
24h
48h
96h
384h
768h
PF (mW/K$^2$m)
0.30
0.25
0.20
0.15
0.10
0.05
0
100
200
300
400
500
600
700
T (ºC)